

Selected recent results on charm hadronic decays from BESIII

HAJIME MURAMATSU

*School of Physics and Astronomy
University of Minnesota, Minneapolis, Minnesota 55455, USA*

I report BESIII preliminary results on:

1. Measurement of $\sigma(e^+e^- \rightarrow D\bar{D})$ at $E_{\text{cm}} = 3.773$ GeV
2. Study of the $D\bar{D}$ production line shape near $E_{\text{cm}} = 3.773$ GeV
3. The first observation of singly Cabibbo-suppressed decay, $D \rightarrow \omega\pi$
4. Measurement of $\mathcal{B}(D_S^+ \rightarrow \eta' X)$ and $\mathcal{B}(D_S^+ \rightarrow \eta' \rho^+)$.

PRESENTED AT

The 7th International Workshop on Charm Physics
(CHARM 2015)
Detroit, MI, 18-22 May, 2015

1 Hadronic decays of charm mesons

Studies of hadronic decays of charm mesons play an important role in the understanding the weak interactions at the c -sector and provide inputs for the beauty physics. Two of samples accumulated by the BESIII detector [1] that are taken at $E_{\text{cm}} = 3.773$ GeV and 4.009 GeV are very useful to study decays of D and D_S^\pm mesons.

The former is the largest e^+e^- annihilation sample in the world to date, 2.92 fb^{-1} [2], that is taken around the nominal mass of $\psi(3770)$ resonance which predominantly decays into a pair of D mesons. The latter, consisting of 482 pb^{-1} [3], also produces a pair of $D_S^+ D_S^-$ with a sizable production rate ($\sigma(e^+e^- \rightarrow D_S^+ D_S^-) \sim 269 \text{ pb}$), providing a clean event environment to study decays of D_S^\pm .

In this proceeding, I report four preliminary measurements from the BESIII collaboration based on the above two e^+e^- annihilation data. The first two results are studies about D -pair productions at the vicinity of the $\psi(3770)$ resonance, a measurement of observed $\sigma(e^+e^- \rightarrow D\bar{D})$ at $E_{\text{cm}} = 3.773$ GeV and a study of Born-level line shape of $\sigma(e^+e^- \rightarrow D\bar{D})$. I then present the first observation of the singly Cabibbo-suppressed decays (SCSD), $D \rightarrow \omega\pi$, and end this report with the measurements of $\mathcal{B}(D_S^+ \rightarrow \eta' X)$ and $\mathcal{B}(D_S^+ \rightarrow \eta' \rho^+)$.

2 $\sigma(e^+e^- \rightarrow D\bar{D})$ at $E_{\text{cm}} = 3.773$ GeV

Measuring observed $\sigma(e^+e^- \rightarrow D\bar{D})$ allows us to estimate the number of $D\bar{D}$ pairs produced in our sample by using the integrated luminosity of the corresponding sample [2]. This can then be used to normalize the measured signal yields to obtain a branching fraction.

As done by the CLEO collaboration [4], we measure the observed cross section by a double-tag technique, pioneered by the MARK III Collaboration [5]. This takes advantage of the fact that D -meson production near the $\psi(3770)$ resonance is solely through $D\bar{D}$.

Reconstructing one D meson in the pair provides a single-tag yield, N_{ST}^i , with a final state, i . We seek 9 different final states: $D^0 \rightarrow (K^-\pi^+, K^-\pi^+\pi^0, K^-\pi^+\pi^+\pi^-)$, and $D^+ \rightarrow (K^-\pi^+\pi^+, K^-\pi^+\pi^+\pi^0, K_S^0\pi^+, K_S^0\pi^+\pi^0, K_S^0\pi^+\pi^+\pi^-, K^+K^-\pi^+)$. (Unless otherwise noted, charge conjugate modes are implied throughout this report.) The detail reconstruction criteria can be found in other BESIII publications, such as Ref. [6].

N_{ST}^i can be written as $N_{ST}^i = N_{D\bar{D}} \cdot \mathcal{B}(D \rightarrow i) \cdot \epsilon_i$, where $N_{D\bar{D}}$ is the number of $D\bar{D}$ produced and ϵ_i is the reconstruction efficiency for the decay mode, $D \rightarrow i$. Similarly, one can have $N_{ST}^j = N_{D\bar{D}} \cdot \mathcal{B}(D \rightarrow j) \cdot \epsilon_j$. When the pair decays explicitly into two final states, $D \rightarrow i$ and $\bar{D} \rightarrow j$, we have $N_{DT}^{ij} = N_{D\bar{D}} \cdot \mathcal{B}(D \rightarrow i) \cdot \mathcal{B}(\bar{D} \rightarrow j) \cdot \epsilon_{ij}$. Here, N_{DT}^{ij} is the *double tag* yield when we simultaneously reconstruct the two mesons in

the final states of i and j . ϵ_{ij} is the corresponding reconstruction efficiency. Solving these for $N_{D\bar{D}}$, one arrives at;

$$N_{D\bar{D}} = \frac{N_{ST}^i \cdot N_{ST}^j \cdot \epsilon_{ij}}{N_{DT}^{ij} \cdot \epsilon_i \cdot \epsilon_j}.$$

The observed cross section is readily obtained by dividing $N_{D\bar{D}}$ by the total integrated luminosity.

We obtain N_{ST}^i from distributions of beam-constrained mass, M_{BC} , defined as $M_{BC} \equiv \sqrt{E_{\text{beam}}^2 - |\vec{p}_D|^2}$. Figure 1 shows fits to M_{BC} distributions based on singly tagged events for the 9 different final states. We use a signal shape predicted by Monte Carlo (MC) simulation. Each of these are convoluted with a Gaussian to take into account a discrepancy in resolution between data and MC, while using an ARGUS background function [7] to represent the background component.

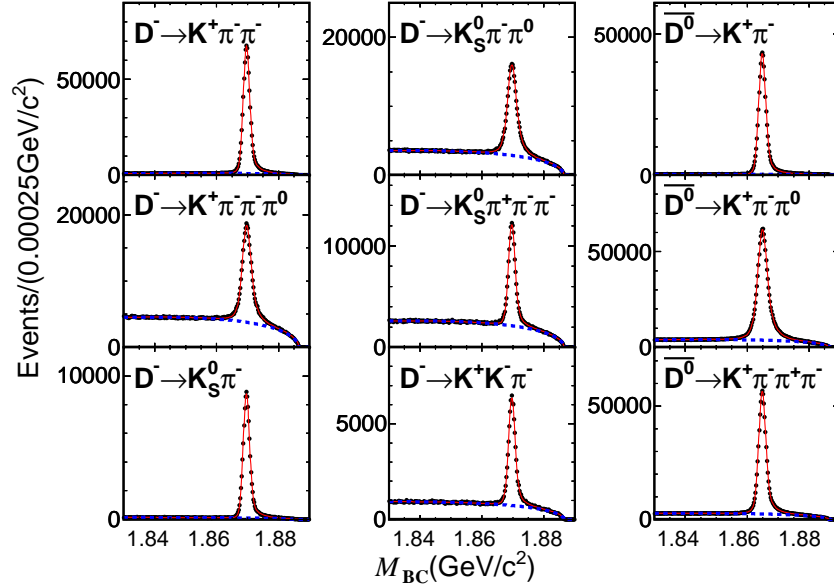


Figure 1: Fits to M_{BC} distributions of singly tagged events based on the entire $\psi(3770)$ sample. Red curves represent the overall fitted shapes and blue dashed curves correspond to the fitted ARGUS background functions.

As for obtaining N_{DT}^{ij} , we look at a two-dimensional space, M_{BC}^i vs M_{BC}^j . Due to the small background of the doubly tagged events, we simply count the yields after using the sidebands of M_{BC} to estimate backgrounds.

Averaging the resultant observed cross sections over different final states ($D \rightarrow j$ and $\bar{D} \rightarrow j$), we have our preliminary result shown in Table 1. Our cross sections are consistent with the ones measured by the CLEO collaboration [4]. We expect our final results to be dominated by systematic uncertainties.

Experiment	$\sigma(e^+e^- \rightarrow D^0\bar{D}^0)$ (nb)	$\sigma(e^+e^- \rightarrow D^+D^-)$ (nb)
This work	3.641 ± 0.010	2.844 ± 0.011
CLEO [4]	$3.607 \pm 0.017 \pm 0.056$	$2.882 \pm 0.018 \pm 0.042$

Table 1: Comparison of the measured cross sections between the BESIII preliminary results and the ones measured by the CLEO collaboration. Only statistical uncertainties are shown in the BESIII results.

3 Line shape of $\sigma(e^+e^- \rightarrow D\bar{D})$

In the previous section, I report our preliminary result of observed cross section, $\sigma(e^+e^- \rightarrow D\bar{D})$, at $E_{\text{cm}} = 3.773$ GeV. It is of great interest to examine this production line shape near the nominal mass of $\psi(3770)$ resonance. This is done using the BESIII scan data which was taken in 2010, along with the main *on-resonant* $\psi(3770)$ sample, in a range of $3.642 < E_{\text{cm}} < 3.890$ GeV with the total accumulated luminosity of ~ 70 pb $^{-1}$. Such a line shape distribution allows one to extract the $\psi(3770)$ resonance parameters. Table 2 shows some of the recent experimental measurements on the nominal mass of $\psi(3770)$ resonance. There is a definite (and expected) shift in the mass when an interference effect is taken into account.

Experiment	$M_{\psi(3770)}$ (MeV/ c^2)
BES (2008) [8]	3772.0 ± 1.9
Belle (2008) [9]	$3776.0 \pm 5.0 \pm 4.0$
<i>BABAR</i> (2007) [10]†	$3778.8 \pm 1.9 \pm 0.9$
<i>BABAR</i> (2008) [11]	$3775.5 \pm 2.4 \pm 0.5$
KEDR (2012) [12]†	$3779.2^{+1.8+0.5+0.3}_{-1.7-0.7-0.3}$

† includes interference

Table 2: Recent experimental measurements on the mass of the $\psi(3770)$ resonance.

To obtain the resonance parameters, we follow the procedure carried out by the KEDR collaboration [12] in which we assume that there are two sources that produce $D\bar{D}$ final states: one from the decay of $\psi(3770)$ and the other from non- $\psi(3770)$ decays. To represent the non- $\psi(3770)$ decays, we form its amplitude as a linear combination of a constant term, which represents the possible contributions from higher $c\bar{c}$ resonant states such as $\psi(4040)$, and a Breit-Wigner form, that corresponds to the $\psi(3686)$ tail above the $D\bar{D}$ mass threshold [13]. This approach is known as a Vector-Dominance Model (VDM), but we also try an exponential form, instead of the Breit-Wigner form, to see how much an alternate form affects the resultant $\psi(3770)$ resonance parameters.

The Born-level cross section, σ_{born} , and experimentally determined observed cross section, σ_{obs} , are related as:

$$\sigma_{obs}(W) = \int z_{DD}(W\sqrt{1-x})\sigma_{born}(W\sqrt{1-x})F_{ISR}(x, W^2)dx.$$

Here, z_{DD} is a factor for the coulomb interaction for D^+D^- , $F_{ISR}(x, W^2)$ is the ISR radiator [14], and $G(W, W')$ (a Gaussian) is there to take into account the beam spread at the initial $E_{cm} = W$. More details can be found in Ref. [12].

We extract $\sigma_{born}(W)$ based on $\sigma_{obs}(W)$ with the above relation. $\sigma_{obs}(W)$ is based on the singly tagged events by fitting to two-dimensional space, ΔE vs M_{BC} , where $\Delta E \equiv E_D - E_{beam}$ with both signal and background shapes are fixed based on MC samples. As an example, Fig. 2 shows projections onto the M_{BC} axes of such two-dimensional fits at $E_{cm} \sim 3.7735$ GeV (left) and $E_{cm} \sim 3.7984$ GeV (right) based on the sum of the three D^0 decays (see the 3rd column of Fig. 1). Notice that the left plot of Fig. 2 peaks at nominal mass of D^0 , while the right plot of Fig. 2 has a 2nd peak on the higher side. This is due to the larger ISR effect at this particular E_{cm} , which our MC-based signal shape (green) reproduces quite well.

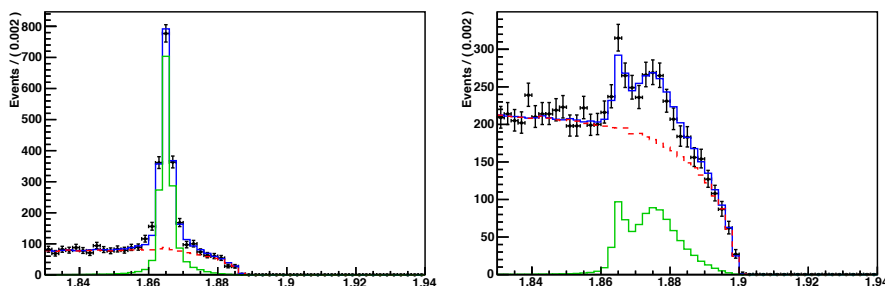


Figure 2: Projections onto the M_{BC} axes (in GeV/c^2) of the two-dimensional fits (ΔE vs M_{BC}) at $E_{cm} \sim 3.7735$ GeV (left) and $E_{cm} \sim 3.7984$ GeV (right) based on the sum of the three D^0 decay modes. The blue histograms represent the overall fits, while dashed red and solid green histograms correspond to the fitted background and signal shapes, respectively.

From these fits at each E_{cm} , we construct the spectrum of the observed cross section, σ_{obs} . As an example, we show σ_{obs} distribution for the case of D^+D^- (red points) in Fig 3. There, the solid blue curve is the fitted shape to σ_{obs} , while the corresponding σ_{Born} is represented by the dashed brown curve. The dashed orange and green curves are the fitted resonant and non-resonant components (here, we use the VDM to represent the non-resonant component).

Table 3 shows our preliminary results on the nominal mass, total width, electronic partial width of the $\psi(3770)$ resonance. The 4th column shows $\Gamma_{ee}^{\psi(3770)} \times \mathcal{B}_{D\bar{D}}$, where $\mathcal{B}_{D\bar{D}} = \mathcal{B}(\psi(3770) \rightarrow D\bar{D})$. This is because our fit is only sensitive to the product of

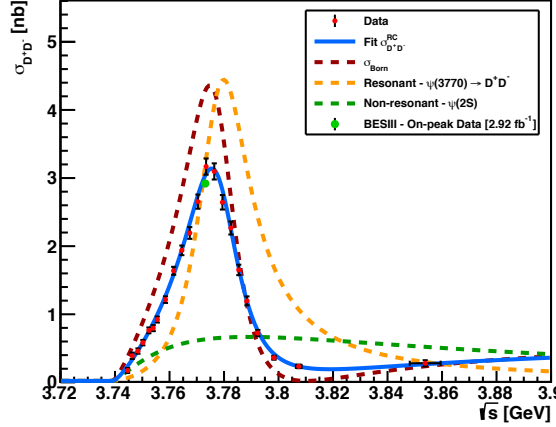


Figure 3: Observed cross section, σ_{obs} is plotted in the red points based on the D^+D^- events in which D^\pm decays into the 6 different final states (see the 1st and the 2nd columns of Fig. 1). The corresponding σ_{Born} curve is shown in dashed brown.

Source	$M^{\psi(3770)}$ (MeV/ c^2)	$\Gamma^{\psi(3770)}$ (MeV)	$\Gamma_{ee}^{\psi(3770)} \times \mathcal{B}_{D\bar{D}}$ (eV)
BESIII _{VDM}	3781.5 ± 0.3	25.2 ± 0.7	230 ± 18
BESIII _{Exponential}	3783.0 ± 0.3	27.5 ± 0.9	270 ± 24
KEDR[12]	$3779.3^{+1.8}_{-1.7}$	$25.3^{+4.4}_{-3.9}$	$160^{+78}_{-58}, 420^{+72}_{-80}$ (a)
PDG[15]	$3773. \pm 0.3$	27.2 ± 1.0	$[262 \pm 18] \times \mathcal{B}_{D\bar{D}}$

(a) Two solutions were obtained from their fit.

Table 3: BESIII preliminary results based on the two different forms of the non- $\psi(3770)$ amplitudes, VDM ($\psi(3686)$) and an exponential shape, are shown, along with the result from the KEDR collaboration as well as the current PDG value. In the 4th column, $\mathcal{B}_{D\bar{D}} = \mathcal{B}(\psi(3770) \rightarrow D\bar{D})$.

the two, but not individually. Our preliminary result is consistent with the KEDR measurement. In Tab. 3 we also show a result based on the exponential form to represent the non- $\psi(3770)$ amplitude. As can be seen, this would likely be one of the dominant sources of the systematic uncertainty.

4 $D \rightarrow \omega\pi$

For Cabibbo-suppressed charm decays, such as the yet to be observed SCSD $D \rightarrow \omega\pi$, measurements are difficult due to low signal statistics and high backgrounds. For the case of $D \rightarrow \omega\pi$, the most recent experimental search was carried out by the CLEO collaboration [16]. They set upper limits, $\mathcal{B}(D^+ \rightarrow \omega\pi^+) < 3.0 \times 10^{-4}$ and

$\mathcal{B}(D^0 \rightarrow \omega\pi^0) < 2.6 \times 10^{-4}$ at 90% confidence level (C.L.). In the mean time, H. Y. Cheng and C. W. Chiang predict the $\mathcal{B}(D \rightarrow \omega\pi)$ could be at an order of 1×10^{-4} [17].

We start with reconstructing one of the $D\bar{D}$ pairs with the same 9 final states (see Fig. 1). Then in the other D decay, we look for $D^{+(0)} \rightarrow \omega\pi^{+(0)}$, where $\omega \rightarrow \pi^+\pi^-\pi^0$ and $\pi^0 \rightarrow \gamma\gamma$. To improve the signal-to-noise ratio, we also select a certain range on the helicity-like angle of ω , θ_{helicity} , which is defined as an opening angle between the direction of the normal to the $\omega \rightarrow \pi^+\pi^-\pi^0$ plane and the direction of the parent D meson in the ω rest frame. We require $|H_\omega| = |\cos \theta_{\text{helicity}}| > 0.54(0.51)$ for D^+ (D^0) that are optimized based on a MC study.

With additional requirements on M_{BC} and ΔE to be consistent with a $D\bar{D}$ pair production, we extract our signal yields by fitting to the distributions of invariant mass of $\omega \rightarrow \pi^+\pi^-\pi^0$ as shown in Fig. 4. We use MC-based signal shapes, along with polynomials to represent their background shapes. Figure 4 also shows the expected peaking backgrounds (represented by filled histograms) which are estimated by the sidebands of M_{BC} distributions. The extracted signal yields correspond to a statistical significance of $5.4\sigma(4.1\sigma)$ for $D^+(D^0) \rightarrow \omega\pi^+(\pi^0)$, respectively.

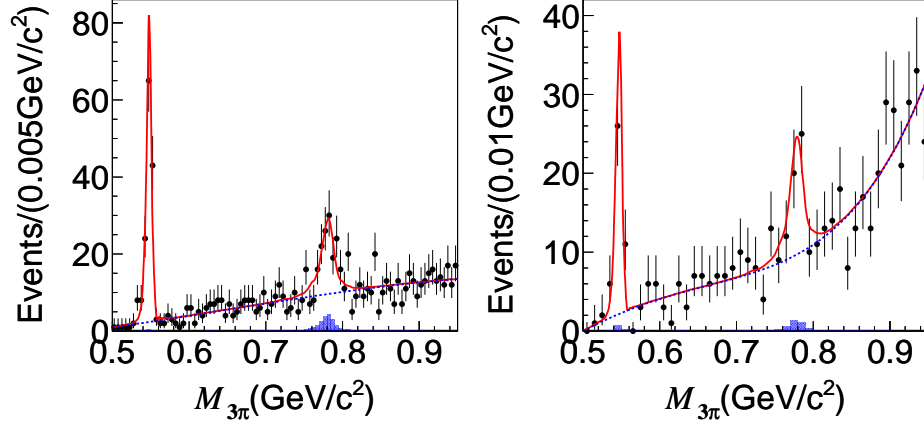


Figure 4: Distributions of invariant mass of $\omega \rightarrow \pi^+\pi^-\pi^0$ for $D^+ \rightarrow \pi^+\pi^-\pi^0\pi^+$ (left) and $D^0 \rightarrow \pi^+\pi^-\pi^0\pi^0$. The solid red lines are the overall fits, while the dashed blue lines represent the fitted polynomials. The filled histograms represent the peaking backgrounds, estimated by the sidebands of M_{BC} distributions.

We also check to see if the $D \rightarrow \omega\pi$ candidates produce the expected distribution of the helicity angle. Figure 5 shows the distributions of $|H_\omega|$ in which we can see the expected $H_\omega^2 = \cos^2 \theta_{\text{helicity}}$.

In Fig. 4, we can also see peaks that correspond to $D \rightarrow \eta\pi$ candidates. We extract these candidates by fitting to the same invariant mass distributions of $\omega \rightarrow \pi^+\pi^-\pi^0$ with much narrower fit ranges, and without the requirement on the $|H_\omega|$. Figure 6 shows such fits from which we also measure $\mathcal{B}(D \rightarrow \eta\pi)$.

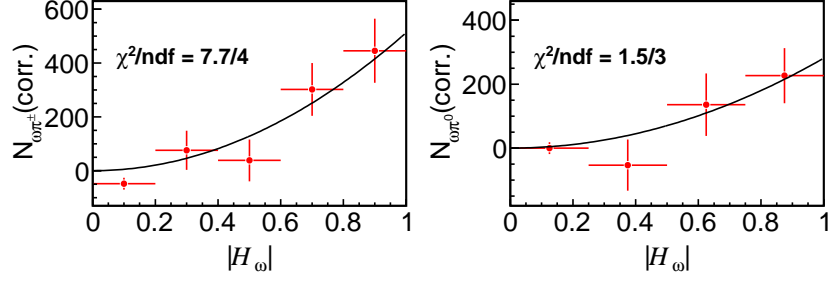


Figure 5: Efficiency-corrected signal yields in the $|H_\omega|$ bins for candidates of $D^+ \rightarrow \omega\pi^+$ (left) and $D^0 \rightarrow \omega\pi^0$ (right). The black lines are the fitted quadratic shapes.

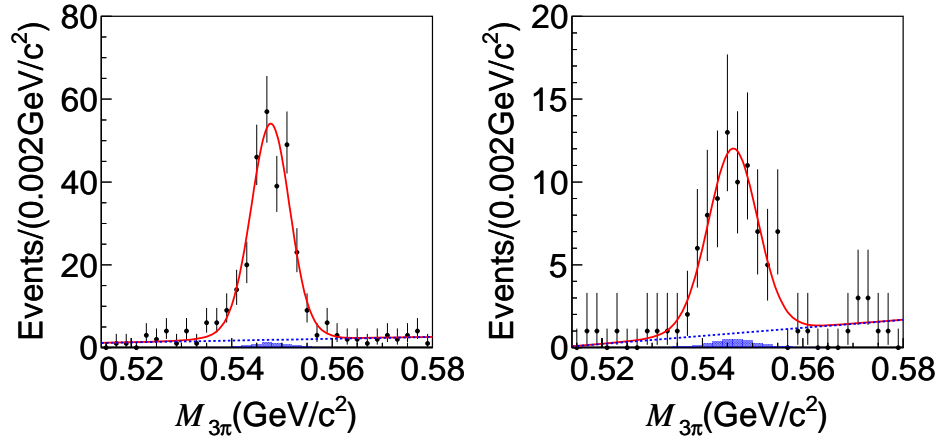


Figure 6: Fits to distributions of invariant mass of $\omega \rightarrow \pi^+\pi^-\pi^0$ for the candidates of $D^+ \rightarrow \eta\pi^+$ (left) and $D^0 \rightarrow \eta\pi^0$ (right). The filled histograms represent the peaking backgrounds which are estimated by the sideband regions of both signal and tag sides of M_{BC} distributions.

Table 4 shows our preliminary branching fraction measurements. The measured $\mathcal{B}(D \rightarrow \eta\pi)$ are consistent with the known values [15], while $\mathcal{B}(D \rightarrow \omega\pi)$ are measured for the first time.

5 $D_S^+ \rightarrow \eta X$ and $D_S^+ \rightarrow \eta\rho^+$

The situation of $\mathcal{B}(D_S^+ \rightarrow \eta'\rho^+)$ is rather interesting. If we sum the all known exclusive rates with η' in D_S^+ decays in the PDG [15], we arrive at $(18.6 \pm 2.3)\%$, while $\mathcal{B}(D_S^+ \rightarrow \eta'X) = (11.7 \pm 1.7)\%$ [18]. Among the D_S^+ decays that involve η' , the largest single exclusive rate is $\mathcal{B}(D_S^+ \rightarrow \eta'\rho^+) = (12.5 \pm 2.2)\%$ [19]. However, a recent measurement is about a half of it, $\mathcal{B}(D_S^+ \rightarrow \eta'\pi^+\pi^0) = (5.6 \pm 0.5 \pm 0.6)\%$ [20] which appears to

Decay mode	This work	PDG value[15]
$D^+ \rightarrow \omega\pi^+$	$(2.74 \pm 0.58 \pm 0.17) \times 10^{-4}$	$< 3.4 \times 10^{-4}$ at 90% C.L.
$D^0 \rightarrow \omega\pi^0$	$(1.05 \pm 0.41 \pm 0.09) \times 10^{-4}$	$< 2.6 \times 10^{-4}$ at 90% C.L.
$D^+ \rightarrow \eta\pi^+$	$(3.13 \pm 0.22 \pm 0.19) \times 10^{-4}$	$(3.53 \pm 0.21) \times 10^{-3}$
$D^0 \rightarrow \eta\pi^0$	$(0.67 \pm 0.10 \pm 0.05) \times 10^{-4}$	$(0.68 \times 0.07) \times 10^{-3}$

Table 4: Preliminary result on the measured $\mathcal{B}(D \rightarrow \omega\pi)$.

solve the inconsistency mentioned above. B. Bhattacharya and J. L. Rosner come up with two predictions, $\mathcal{B}(D_S^+ \rightarrow \eta'\rho^+) = (2.9 \pm 0.3)\%$ and $(1.89 \pm 0.20)\%$ [21], while F. S. Yu *et al.* predict $(3.0 \pm 0.5)\%$ [22] by factorization methods.

We can use our sample taken at $E_{\text{cm}} = 4.009$ GeV to measure these branching fractions to confirm the recent measurement. At this energy, the D_S^\pm is produced in a pair. To measure the inclusive rate, $D_S^+ \rightarrow \eta'X$, we employ a double-tag technique in which we reconstruct its tag side in 9 decay modes shown in Fig. 7. From these M_{BC} distributions, the single-tag yields are readily obtained.

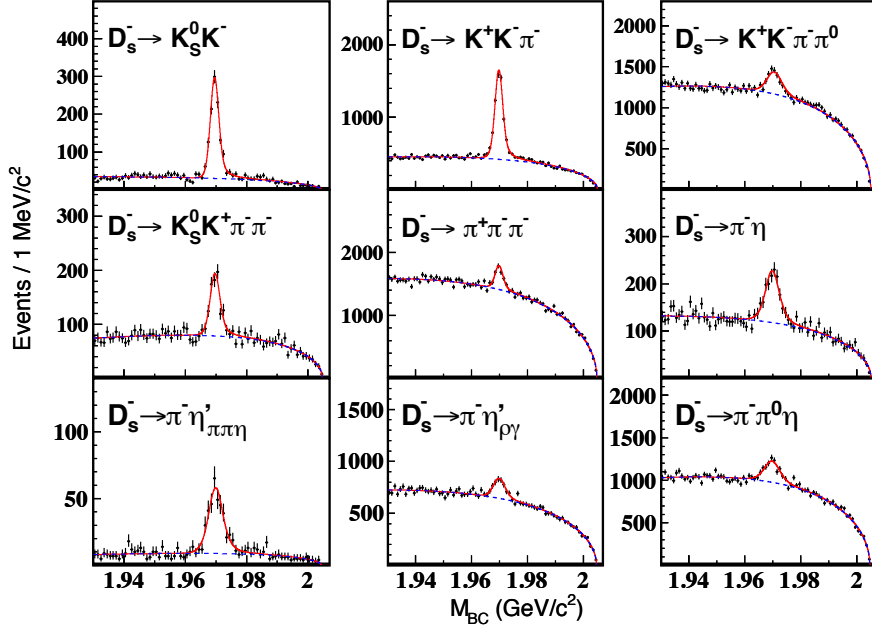


Figure 7: Fits to M_{BC} distributions of the selected 9 different final states of D_S^+ decays. The red curves correspond to the total fits, while the blue dashed curves represent the fitted background shapes by the ARGUS background functions [7].

To obtain the double-tag yields, we reconstruct the 9 final states of D_S^\pm decays and look for the other D_S^\mp decays in the final states with $\eta' \rightarrow \pi^+\pi^-\eta(\rightarrow \gamma\gamma)$ based

on the remaining particles. If there is more than one η' candidate, we choose the one that gives the minimum $|M_{\pi^+\pi^-\eta} - M_{\eta'}(PDG)|$. We fit to a two-dimensional space, $M_{\pi^+\pi^-\eta}$ vs M_{BC} , to extract the signal yields, where M_{BC} is the tag side of the beam-constrained mass. Figure 8 shows such fits, projected onto the M_{BC} axis (left) and onto the $M_{\pi^+\pi^-\eta}$ axis (right). We use MC-based distributions to represent the signal shape. As for the background shapes, an ARGUS background function [7] is used on the M_{BC} direction, while the smooth and peaking backgrounds on the $M_{\pi^+\pi^-\eta}$ axis are represented by a polynomial plus double Gaussian shapes.

From this fit, 68 ± 14 events are observed as signal candidates. This translates into $\mathcal{B}(D_S^+ \rightarrow \eta' X) = (8.8 \pm 1.8 \pm 0.5)\%$ which agrees with the known value [15].

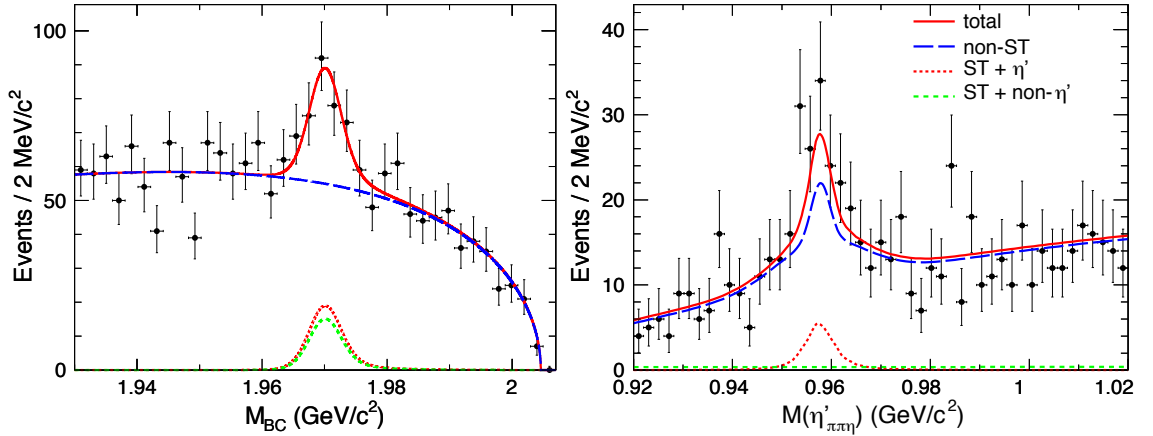


Figure 8: Fit to two-dimensional space, $M_{\pi^+\pi^-\eta}$ vs M_{BC} , where M_{BC} is the tag side of the beam-constrained mass. Shown here are the fitted result, projected onto the M_{BC} axis (left) and onto the $M_{\pi^+\pi^-\eta}$ axis (right). Solid red curves correspond to the overall fit, while dashed blue and green curves are fitted peaking backgrounds.

To measure $\mathcal{B}(D_S^+ \rightarrow \eta' \rho^+)$, we simply use the single-tag method by reconstructing $D_S^+ \rightarrow \eta' \rho^+$, where $\rho^+ \rightarrow \pi^+ \pi^0$. We require the reconstructed η' mass to be within 3σ of the known mass [15], the invariant mass $M_{\pi^+\pi^0}$ be within $0.17 \text{ GeV}/c^2$ of the known ρ mass [15], and finally its ΔE be consistent with zero.

The signal yield is extracted by fitting to two-dimensional space, M_{BC} vs $\cos \theta_{\pi^+}$, where θ_{π^+} is the helicity angle of the π^+ from the ρ decay. We expect to see $\cos^2 \theta_{\pi^+}$ for $D_S^+ \rightarrow \eta' \rho^+$, while $D_S^+ \rightarrow \eta' \pi^+ \pi^0$ events should be independent of θ_{π^+} .

Figure 9 shows projections onto the M_{BC} axis (left) of such two dimensional fit. On the right, a projection onto the $\cos \theta_{\pi^+}$ axis with an additional requirement of $(1.960 < M_{BC} < 1.980) \text{ GeV}/c^2$ is shown. Signal shapes are based on MC simulation. To represent the background shapes, an ARGUS background function [7] is used on the M_{BC} axis, while a fixed non- D_S^+ background shape is employed on the $\cos \theta_{\pi^+}$ axis, estimated from the M_{BC} sidebands.

The fit yields 210 ± 50 and -13 ± 56 events for $D_S^+ \rightarrow \eta' \rho^+$ and $D_S^+ \rightarrow \eta' \pi^+ \pi^0$ candidates, respectively. We normalize the rate by $D_S^+ \rightarrow K^+ K^- \pi^+$ mode to obtain $\mathcal{B}(D_S^+ \rightarrow \eta' \rho^+)/\mathcal{B}(D_S^+ \rightarrow K^+ K^- \pi^+) = 1.04 \pm 0.25 \pm 0.07$. Or with the known $\mathcal{B}(D_S^+ \rightarrow K^+ K^- \pi^+)$ [15], we arrive at $\mathcal{B}(D_S^+ \rightarrow \eta' \rho^+) = (5.8 \pm 1.4 \pm 0.4)\%$ which confirms the recent measurement by the CLEO collaboration [20]. We also set an upper limit on the non-resonant decay, $\mathcal{B}(D_S^+ \rightarrow \eta' \pi^+ \pi^0) < 5.1\%$ at 90% C.L.

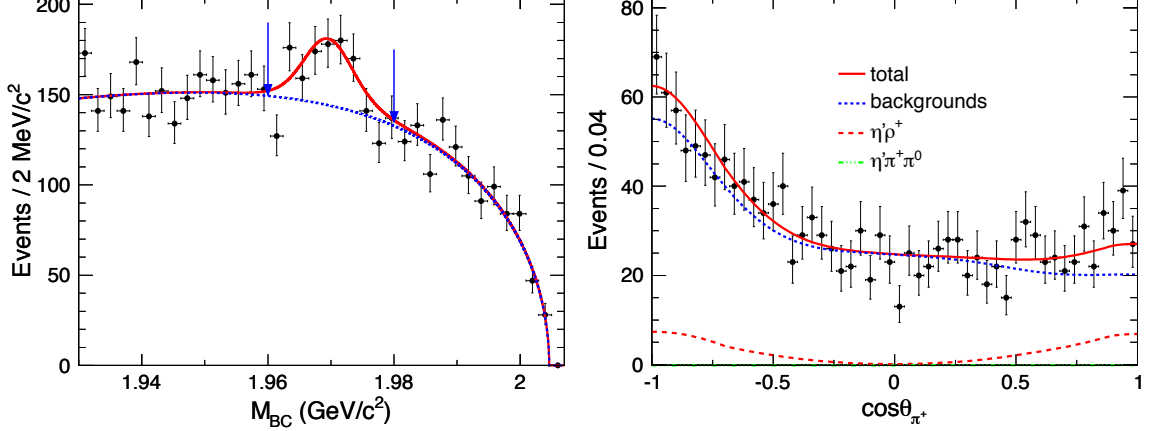


Figure 9: Projections onto the M_{BC} axis (left) and the $\cos \theta_{\pi^+}$ axis with an additional requirement of $(1.960 < M_{BC} < 1.980)$ GeV/c^2 (right) of the two-dimensional fit.

6 Conclusion

Four preliminary results on the hadronic final states in the decays of D and D_S^\pm mesons based on the two recent BESIII samples are reported. The measurements based on the world's largest e^+e^- annihilation sample taken at $E_{\text{cm}} = 3.773$ GeV provide statistically superior results than the previous experimental results, while the study of decays of D_S^\pm based on the sample at $E_{\text{cm}} = 4.009$ GeV shows the very clean event environment at BESIII. It would be very exciting to pursue our D_S program as the collaboration plans to take a few fb^{-1} of e^+e^- annihilation sample at $E_{\text{cm}} = 4.180$ GeV in 2015 – 2016, where the production rate of D_S^\pm is much higher, $\sigma(e^+e^- \rightarrow D_S^{*\pm} D_S^\mp) \sim 900$ pb.

ACKNOWLEDGEMENTS

I would like to thank Derrick Toth, Andy Julin, Xiaoshuai Qin, and Peilian Liu for preparing and providing the figures and comments.

References

- [1] M. Ablikim *et al.* (BESIII Collaboration), [Nucl. Instrum. Methods Phys. Res., Sec. A **614**, 345 \(2010\)](#).
- [2] M. Ablikim *et al.* (BESIII Collaboration), [Chin. Phys. C **37**, 123001 \(2013\)](#).
- [3] M. Ablikim *et al.* (BESIII Collaboration), [Chin. Phys. C **39**, 093001 \(2015\)](#).
- [4] G. Bonvicini *et al.* (CLEO Collaboration), [Phys. Rev. D **89**, 072002 \(2014\)](#).
- [5] R. M. Baltrusaitis *et al.* (MARK III Collaboration), [Phys. Rev. Lett. **56**, 2140 \(1986\)](#).
- [6] M. Ablikim *et al.* (BESIII Collaboration), [Phys. Lett. B **744**, 339 \(2015\)](#).
- [7] H. Albrecht *et al.* (ARGUS Collaboration), [Phys. Lett. B **241**, 278 \(1990\)](#).
- [8] M. Ablikim *et al.* (BES Collaboration), [Phys. Lett. B **600**, 315 \(2008\)](#).
- [9] J. Brodzicka *et al.* (Belle Collaboration), [Phys. Rev. Lett. **100**, 092001 \(2008\)](#).
- [10] B. Aubert *et al.* (*BABAR* Collaboration), [Phys. Rev. D **76**, 111105\(R\) \(2007\)](#).
- [11] B. Aubert *et al.* (*BABAR* Collaboration), [Phys. Rev. D **77**, 011102\(R\) \(2008\)](#).
- [12] V.V. Anashin *et al.* (KEDR Collaboration), [Phys. Lett. B **711**, 292 \(2012\)](#).
- [13] Hai-Bo Li, Xiao-Shuai Qin, and Mao-Zhi Yang, [Phys. Rev. D **81**, 011501\(R\) \(2010\)](#); Yuan-Jiang Zhang and Qiang Zhao, [Phys. Rev. D **81**, 034011 \(2010\)](#).
- [14] E.A. Kuraev, V.S. Fadin, [Sov. J. Nucl. Phys. **41**, 466 \(1985\)](#).
- [15] K. A. Olive *et al.* (Particle Data Group), [Chin. Phys. C **37**, 090001 \(2014\)](#).
- [16] P. Rubin *et al.* (CLEO Collaboration), [Phys. Rev. Lett. **96**, 081802 \(2006\)](#).
- [17] Hai-Yang Cheng and Cheng-Wei Chiang, [Phys. Rev. D **81**, 074021 \(2010\)](#).
- [18] S. Dobbs *et al.* (CLEO Collaboration), [Phys. Rev. D **79**, 112008 \(2009\)](#).
- [19] C. P. Jessop *et al.* (CLEO Collaboration), [Phys. Rev. D **58**, 052002 \(1998\)](#).
- [20] P. U. E. Onyisi *et al.* (CLEO Collaboration), [Phys. Rev. D **88**, 032009 \(2013\)](#).
- [21] B. Bhattacharya and J. L. Rosner, [Phys. Rev. D **79**, 034016 \(2009\)](#).
- [22] Fu-Sheng Yu, Xiao-Xia Wang, and Cai-Dian Lü, [Phys. Rev. D **84**, 074019 \(2011\)](#).